Assessing the Impact of Membrane Deformations on Wing Sail Performance

Joseph Banks
University of Southampton, UK, J.Banks@soton.ac.uk

Margot Cocard
University of Strathclyde, UK.

Jacobo Jaspe
One Fluid, Spain.

Abstract. The aim of this research is to quantify the membrane deformations and their impact on performance for a ribbed wing sail. A 1m x 0.8m rectangular planform NACA0012 foil was designed to replicate a single section of a wing-sail. Two foils were manufactured based on this geometry, one out of solid foam and one using a rib and membrane structure. These were tested in the R.J. Mitchell closed return 3.6 m x 2.5 m wind tunnel at the University of Southampton. Their aerodynamic performance was assessed over a range of angles of attack using a six-component force balance showing the overall performance of the membrane wing was reduced by between 5-11% depending on the analysis conducted. A stereo camera system was used to perform Digital Image Correlation (DIC) in order to quantify the full field deformation of the membrane wing structure whilst under aerodynamic load. This showed membrane deformations of up to 15% of the section thickness. The experimental membrane displacements were then used to create a deformed wing sail geometry, removing the effect of foil bend and twist, allowing a CFD investigation of the impact of membrane deformations alone. This indicated that the static membrane deformations resulted in a decrease in performance of up to 1.3% compared to the rigid aerofoil.

Keywords: membrane deformation; fluid structure interaction; wind tunnel; CFD; DIC; wing sail.

NOMENCLATURE

L	Lift Force [N]
D	Drag Force [N]
C_L	Lift Coefficient [-]
C_D	Drag Coefficient [-]
C_P	Pressure Coefficient [-]
C_L/C_D	Foil performance [-]
$\propto$ or AoA	Angle of Attack [deg]
V	Wind Speed [m/s]

CFD	Computational Fluid Dynamics
DIC	Digital Image Correlation
FSI	Fluid Structure Interactions

1. INTRODUCTION

Recent years have seen an increase in the use of wing-sails for sailing applications including previous America's Cup yachts and wind assisted commercial vessels. These structures provide a higher lift to drag ratio then traditional sails (Haack, 2018). They also provide an increased level of control over the wing shape and therefore the forces generated. However, these advantages come with a weight penalty so the wing sails used in competitive racing need to be made as light as possible. This is typically achieved by building a ribbed structure that creates the desired aerodynamic shape and stretching a flexible membrane over it. This creates a very efficient structure, similar to those used for lightweight unmanned aerial vehicles. However, it is unclear what impact the membrane deformations have on the aerodynamic performance of the wing-sail. Given how traditional sails change their shape significantly due to aerodynamic loading (Deparday *et al*, 2016; Ramolini, 2019) and their performance is significantly affected by fluid structure interactions (Aubin *et al*, 2017) it seems likely that membrane deformations will affect the performance of a wing sail.

Initial research into wing sails focused on their structure and control but several studies have investigated their aerodynamic performance and design using CFD (Fiumara *et al* 2016; Fiumara *et al* 2016b; Collie *et al* 2015; Li *et al*, 2020). Wind tunnel tests have also investigated the aerodynamic performance of two section wing sails looking at the impact of the gap between the two elements and Reynolds number effects (Furukawa *et al*, 2015). Whilst the the impact of twist, heel angle and camber distribution has also been investigated in the wind tunnle (Magherini *et al,* 2014). Research has looked at assessing the overall performance of a wing-sailed vessel using Velocity Prediction Programs (VPPs). This has included predicting the steady state performance of a hydrofining catamaran with a wing sail (Hagemeister and Flay, 2019); investigating the control of a wing sail in order to complete successful manoeuvres of a foiling AC50 catamaran using a dynamic VPP (Hansen *et al*, 2019); understanding the impact of different depowering strategies for the use of wing sails on commercial ships (Olsson *et al*, 2020) and even coupling CFD optimisation of wing sail design with overall vessel performance (Viola *et al*, 2015).

Assessing the impact of membrane deformations is a complex Fluid Structure Interaction (FSI) problem to solve numerically due to the coupling required between fluid and structural solvers. Model scale experiments are challenging due to the requirement to correctly scale the structural properties. Therefore, very little research has been published into the impact of membrane deformations on wing sail performance in sailing and it is often assumed that the membrane deformations are small enough to neglect at the design stage.

Recent interest in the aerodynamics of animals that use membrane wings, such as bats, flying squirrels but also Jurassic dinosaurs (Pterosaur Pterodactylus) have led researchers to investigate the performance of flexible membrane wings. This interest has varied from developing analytical methods for assessing the impact of membrane stiffness on wing performance (Jackson *et al,* 2001) to a more recent desire to increase the manoeuvrability and reduce weight in Micro Air Vehicles (MAV) and other small aircraft (Arbos Torrent, 2013). Research in this field has shown that membrane wings can have a steeper lift slope as well as higher/smoother stall angles and an overall higher performance due to the fluid structure interaction (Arbos Torrent 2013; Rojratsirikul 2010; Fairuz et al 2016; Gordnier, and Attar, 2014; Bleischwitz et al, 2016). The unsteady effects of the membrane vibrations can also affect separated regions of flow, significantly changing the foil's performance (Rojratsirikul, 2010; Bleischwitz et al, 2017).

Although this research indicates that membrane deformations could have a significant impact on aerodynamic performance, these studies were all conducted on a single membrane acting as a lifting surface. A recent publication looked at the performance of a 3D, double skinned, membrane wing with a solid nose section and a small rigid support for the trailing edge (Piquee et al, 2019). The membrane deformations increased the section camber increasing the lift generated by the wing and helped to smooth out the reduction in lift as stall occurred. This concept, however, is

quite different to the wing sails adopted so far in sailing where the membrane is supported by a ribbed structure to minimise membrane deformations. So far there has been no published research into the magnitude or impact of membrane deformations on an aerofoil shaped ribbed wing sail.

The aim of this research is to quantify the membrane deformations and their impact on performance for a ribbed wing sail. To achieve this, controlled experimental tests of a ribbed membrane wing section were conducted in a wind tunnel section allowing both the structural deformations and the aerodynamic forces to be determined. The impact of the membrane deformations were further investigated using numerical simulations.

2. EXPERIMENTAL INVESTIGATIONS

In order to replicate the structural properties of a full-scale wing sail as closely as possible only a single element of the wing was tested in the wind tunnel. This maximised the size of the membrane panels creating a realistic test case for membrane deformations without needing to scale the structural properties on the membrane.

2.1 Wing Sail Design and Manufacture

Two symmetric NACA 0012 foils, with dimensions 976 mm (span) x 806 mm (chord), were designed to be mounted onto an 102 mm x 25 mm aluminium box section beam attached to the wind tunnel dynamometer. The beam was located at ¼ of the chord back from the leading edge of the foil. One foil had a ribbed structure manufactured out of polystyrene foam, as seen in Figure 1, whilst one was manufactured out of solid foam. As the aim of the research was to investigate membrane deformations no attempt was made to replicate the internal structural properties of the design. The design simply tried to minimise internal structural deformations with limited manufacturing time and budget.

Both foils were covered with a light membrane (a heat shrinkable and printable cross-linked 50 micron thick polyolefin from PROtect tapes). This membrane was selected as the manufacturer has supplied this product for America's Cup wing sails in the past. The membrane was attached to the foil structure and then heated until the maximum pretension was reached.

The entire foil was painted matt black before a speckle pattern, with a speckle size of 2.1mm (approximately 6 pixels) and 60% fill density, was applied to both foils using printable adhesive transfers, as seen in Figure 2. This ensured that both foils had the same surface finish.

2.2 Experimental Method

The experiments were conducted in the R.J. Mitchell wind tunnel facility at the University of Southampton which has a 3.6m wide x 2.5m high x 10.5m long working section and can provide a speed range from 4 to 40 m/s with less than 0.2% turbulence intensity.

The foils were attached to the six degree of freedom Nuntem load cell balance, mounted on a turntable in the roof of the wind tunnel. This placed the aluminium box beam at the centre of rotation on the central axis of the wind tunnel. A small clearance gap was required between the root of the foil and tunnel roof, but this was kept below 5 mm to minimise end effects in this region.

A LaVision stereo DIC system was set up in the wind tunnel viewing room (see Figure 3), comprising of two E-Lite 5M cameras fitted with 28 mm lenses, with a stand-off distance of 2.8m. The speckle pattern was illuminated using four high powered Nila LED spot lights mounted within the working section.

The DIC system was calibrated utilising a LaVision type 309-15 calibration plate using a total of 7 static images with the plate at different orientations within both cameras field of view. This produced a calibration RMS fit error of 0.246, well within the recommended values provided by LaVision.

The Images were recorded with a frame rate of 10 Hz and processed using the LaVision software DaVis using a cross correlation method to provide the surface deformations of the structure. The DIC methodology applied here is based on the methods presented in Banks *et al* (2015) and Marimon Giovannetti (2017) and more detail can be found there.
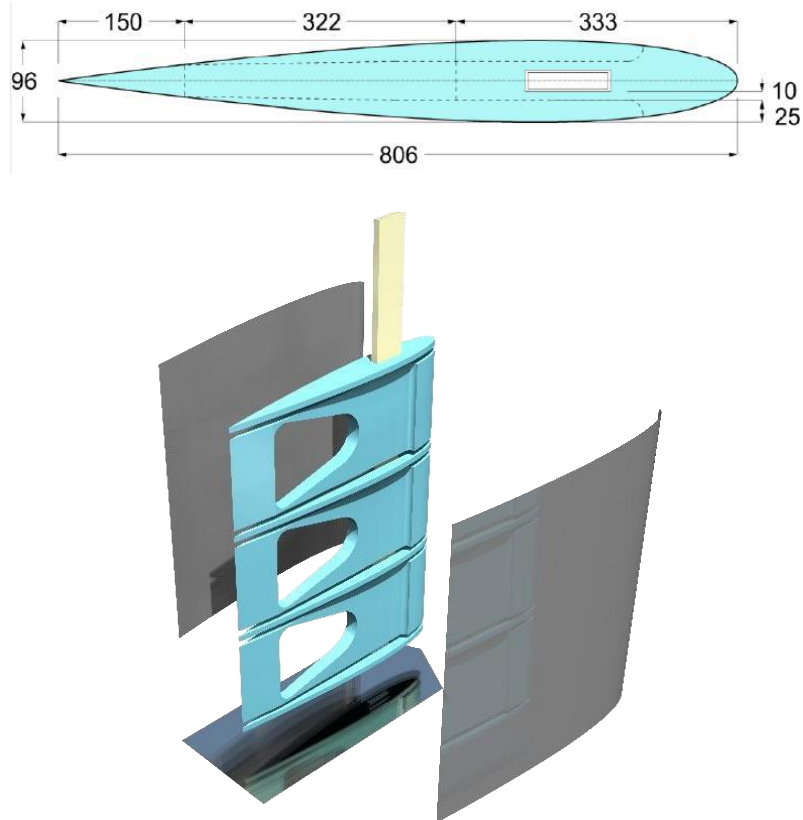

Figure 1 - Foil design for membrane wing, all dimensions provided in mm.

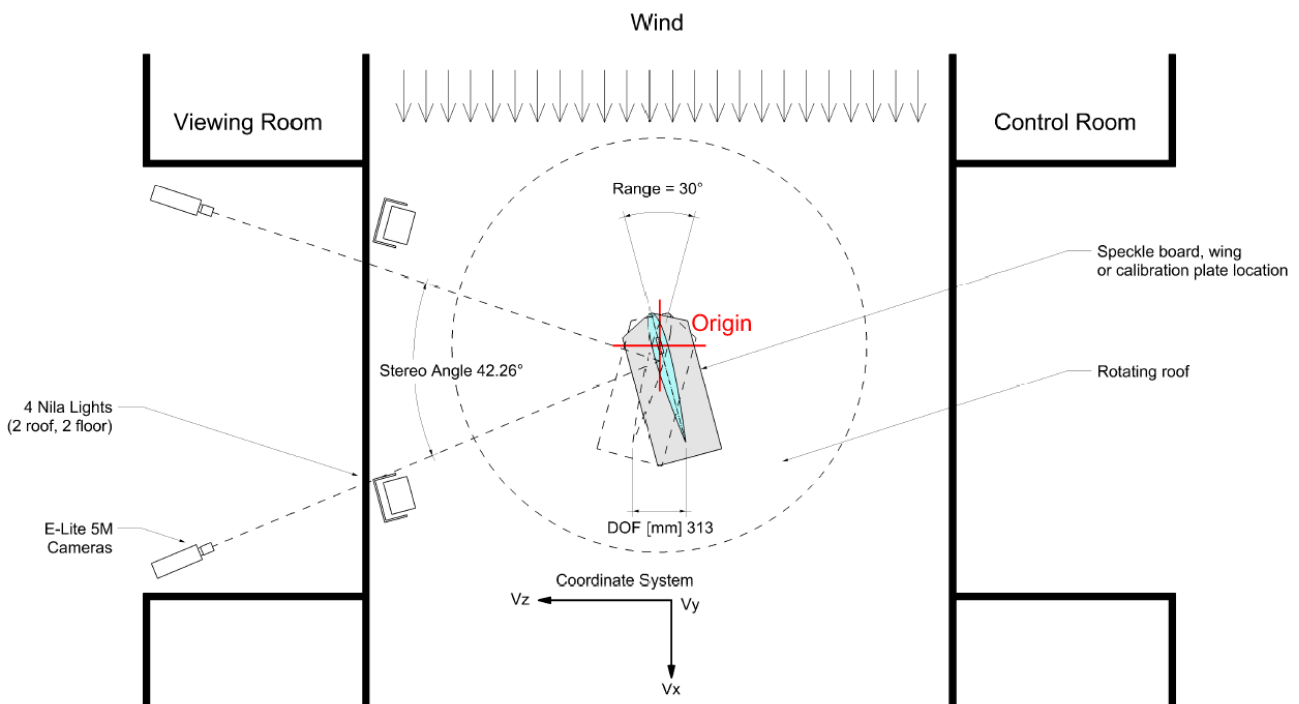**Figure 2 - Speckle pattern applied to solid foil**

Figure 3 - wind tunnel schematic

In order to assess the accuracy of the DIC method a flat plate with the same speckle pattern applied to it was mounted onto a Standa high-precision motorised translation stage (Model 8MT175-50). A series of 10 images were acquired of the specimen in each known displacement varying from 0-50 mm. The DIC software then corelates the images of the displaced specimen with those of the original static specimen to calculate the displacement vector. This is then compared against the known displacement from the stage to provide a percentage error. These tests showed that deformations between 0.1 and 0.5 mm have an out-of-plane error of less than 3% and those above 0.5mm have an error lower than 0.3%. This indicates a much lower error than previous experiments using a similar experimental setup which have shown a significant increase in the error for displacements below 0.5mm (Banks *et al* 2015; Marimon Giovannetti 2017). There is no clear reason why the error in this experiment should be much lower than previously reported indicating further verification of these findings is needed in the future. It appears however that the DIC measurement accuracy is at least as good as previously published data and is suitable for determining membrane deformations in the order of millimetres proposed in this study.

To quantify the impact of membrane deformations over a range of angles of attack a series of test were conducted at reciprocal positive and negative angles of attack (0,±9, ±12 and ±15 degrees) allowing the deformations on both the pressure and suction side to be determined from one side of the wind tunnel. It is therefore assumed that the structural properties of the membrane are the same on both sides of the aerofoil.

The wings were tested at three wind speeds (10, 15 and 20 m/s) covering a range of Reynolds numbers from 0.71 to 1.4 million. This range was effectively defined by the size of the wing that could be tested in the wind tunnel facility and the range of wind speeds that could be used without overloading and potentially damaging the foil structure. This does mean that the flow will transition from laminar to turbulent at different location along the foil at different wind speeds.

2.3 Experimental Results

The full-field deformation data over the bottom two thirds of the tested wing section could be determined from the DIC results. This naturally included any bend and twist of the mounting beam and the internal foam structure as well as the membrane deformations. Despite locating the

77

aluminium beam at approximately the ¼ chord, to minimise the distance between the shear centre of the structure and the aerodynamic centre of effort, noticeable twist deformations were observed at the foil tip. This is likely to be caused by a combination of an aerodynamic torsional moment twisting the beam and local structural deformations of the foam structure along the chord. Therefore, the deformation measured along the foam leading and trailing edges were used to remove these global effects from the deformation field resulting in only the membrane deformation. An example of this data is presented in Figure 4 showing significant membrane deformation inward (towards the foil centreline) on the pressure side of the wing and a mixture of inward and outward deformation on the suction side of the wing. It can be observed that of the two measured membrane panels (separated by foam ribs) the panel located closest to the wing tip exhibits larger deformations with a different distribution then the middle panel of the wing. This is thought to be associated with the end effects of a finite span wing changing the pressure distribution near the wing tip. As the top of the foil is located very close to the wind tunnel roof this should act similar to a reflection plane resulting in a similar pressure distribution and deformation as the middle panel.
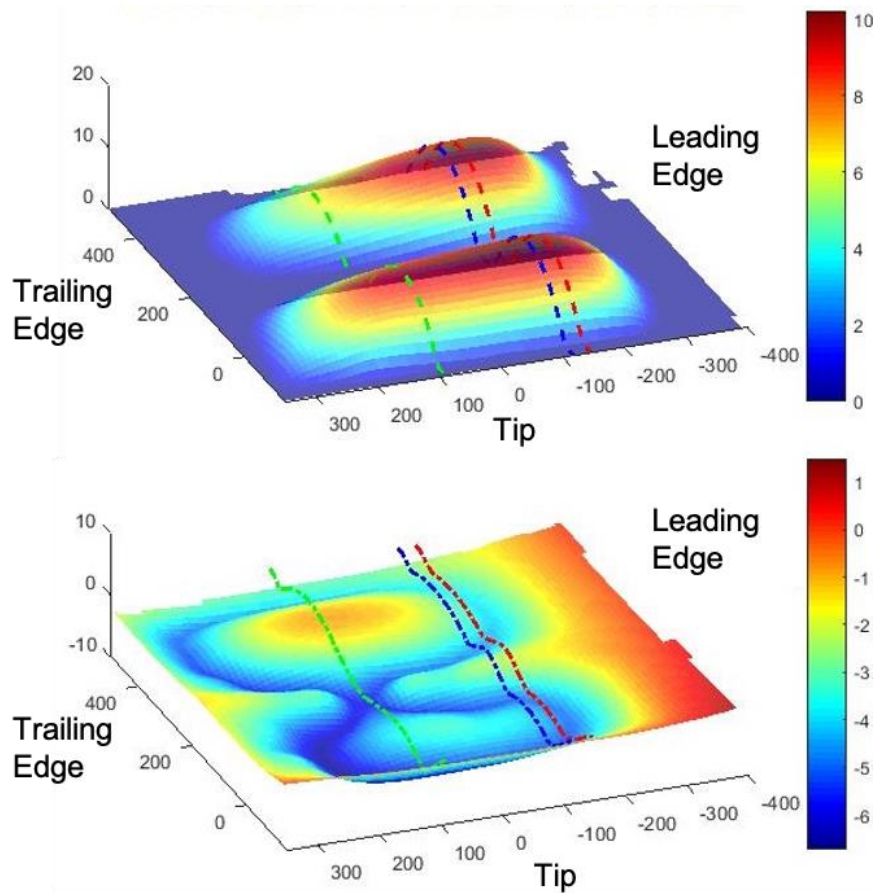

Figure 4 - Membrane deformations in mm normal to the foil's centreline at a wind speed of 20m/s. Deformations for the pressure side of the wing (above) were obtained at an AoA of +12 deg, whilst the suction side (below)were obtained at an AoA of -12 deg. Positive deformations are away from the cameras (see figure 3) and towards the foil centreline.

To provide a representation of the deformed shape of the foil the measured deformations due to aerodynamic load were added to the unloaded shape of the membrane wing, which was determined from the static DIC images (Figure 5 and Figure 6). The effect of the pre-tension within the membrane can easily be observed in Figure 6, where the unloaded surface sags inwards by up to 5 mm from the designed section shape. When exposed to fluid dynamic loading, this increases to a maximum of 15 mm offset (approximately 15% of the section thickness). Combined with the slight outward displacements on the suction side of the foil this alters the section shape considerably in the middle of the membrane panels. In general the membrane remains securely

attached to the foam ribs except in one location (at the chordwise position denoted by the green dashed line in Figure 4Figure 6). When exposed to suction pressures this small region of membrane is sucked out from the foam rib.

It should be highlighted that Figure 5 only represents the regions that DIC data was obtained for, which excludes a region at the leading and trailing edges. Therefore, the measured membrane positions have been offset in Figure 5 to represent the full section thickness.

Visual inspection of the membrane indicated a steady deformed shape with no large vibrations prior to stall. This impression was backed up by multiple deformation measurements for each condition showing a very small standard deviation of the membrane deformations.
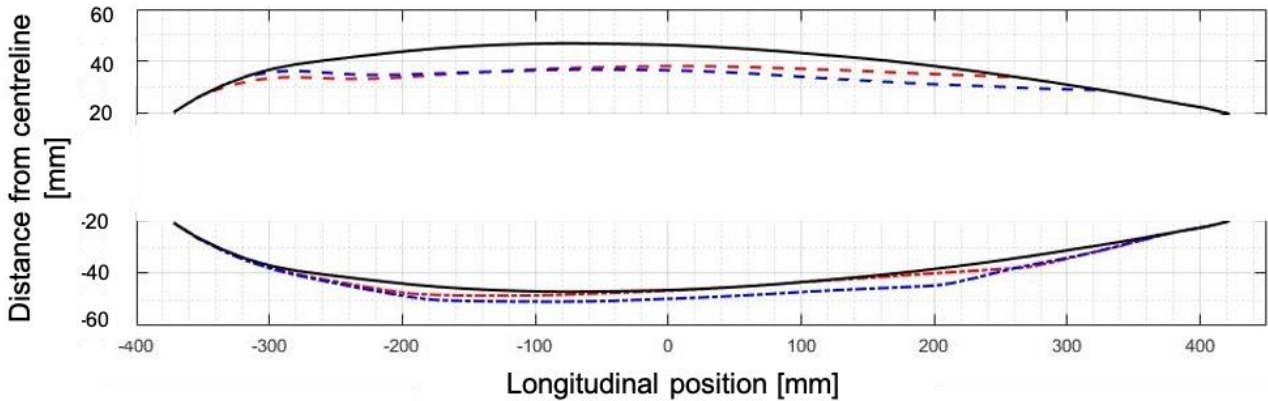

Figure 5 – Measured membrane position (in mm) on a horizontal section midway between two ribs for an AoA of 12 deg. The unloaded membrane position is provided in black and aerodynamic loading at 20 m/s wind speed provided in red (middle panel) and blue (lower panel)
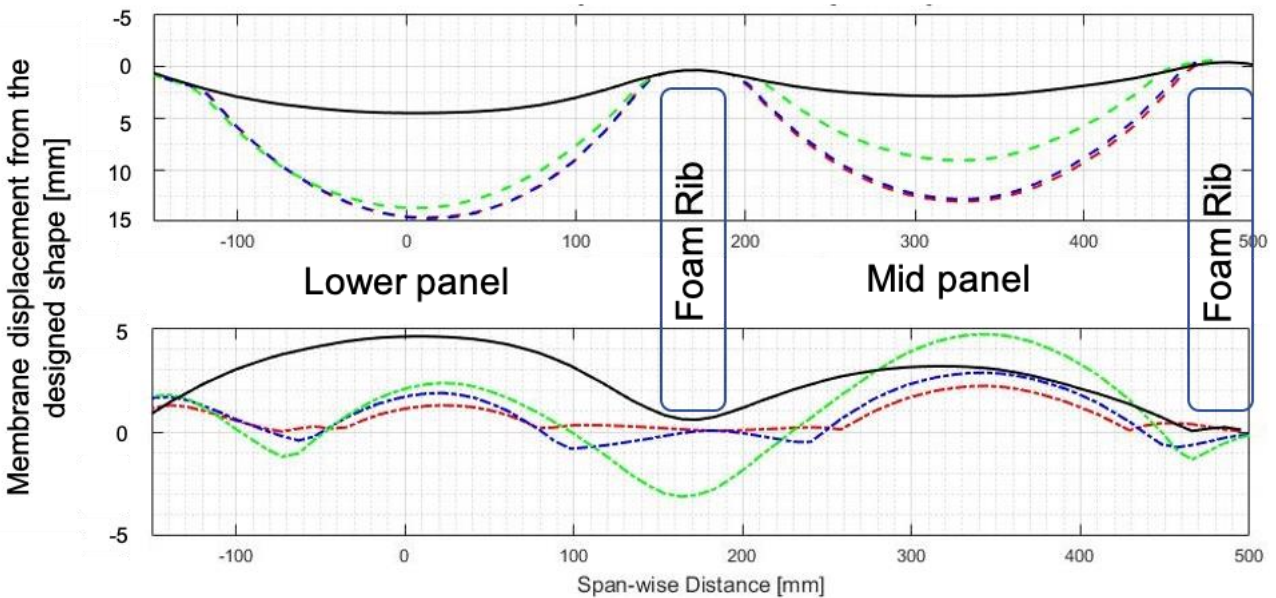

Figure 6 – Span-wise membrane displacement (in mm) relative to the designed section shape for the different chord-wise locations marked in Figure 4, for an AoA of 12 deg. Positive displacements are towards the foil centreline with the pressure side of foil provided above (with an inverted displacement scale) and the suction side of foil provided below. Zero wind speed condition is given in black, 20 m/s condition by dashed lines

The presented membrane deformations are pretty representative of the deformed shape for all the conditions tested. The magnitude of the deformations varied, however, with both angle of attack and wind speed, as seen in Figure 7.
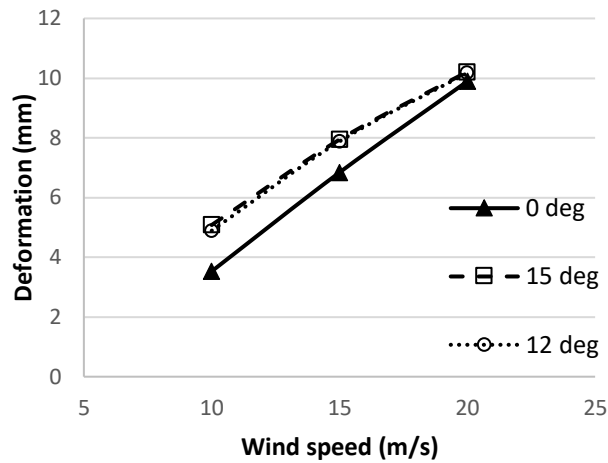

Figure 7 - Maximum membrane deformation for varying AoA and wind speed.

The measured lift and drag coefficients for both the solid and membrane wing are presented in **Figure 8**. We would expect to see a linear increase in lift, and a quadratic increase in drag, with increasing angle of attack until stall. The majority of the data follows this general trend with the exception of the solid foil for positive angles of attack, which produced unusual trends in drag and some indication of stall in the lift forces at lower wind speeds. It is also evident that the data is not completely symmetrical for either foil indicating potential issues with foil alignment. Unfortunately, due to restricted tunnel time and an initial focus on quantifying the membrane deformations, only a limited number of angles of attack were conducted and no repeat conditions. It is therefore unclear whether the unusual forces observed for the solid wing are due to instrumentation or experimental set up issues or physical phenomena associated with the solid foil. Fortunately, the data for the membrane wing does not exhibit the same trends, giving confidence in the deformation measurements, however it is difficult to draw direct comparisons between the solid and membrane wing forces.

Including all the data indicates a 6% reduction in lift and a 1 % reduction in drag, resulting in an overall reduction in lift to drag ratio of 5% for the membrane foil. If, however, we assume that the data obtained for the solid wing at positive angles of attack is untrustworthy and replace this with the force coefficients from the negative angles of attack, a potentially more realistic assessment of performance can be obtained. This results in a 6% reduction in lift and a 6% increase in drag, resulting in a 11% reduction in the lift to drag ratio.

Overall this leads to a significant amount of uncertainty regarding the impact of membrane deformations on foil performance, especially as the observed changes will be in part be due to the observed global deformations of the wing (i.e. bend and twist). The observed twist deformations will have the impact of reducing the angle of attack of the foil towards the tip, reducing the local lift and drag forces in this region.

In order to focus on the impact of membrane deformations alone a method was required to isolate this phenomenon from wider issues of flexible foil performance. As the deformed shape of the membrane wing had been measured it was decided to use numerical simulations to investigate this further.
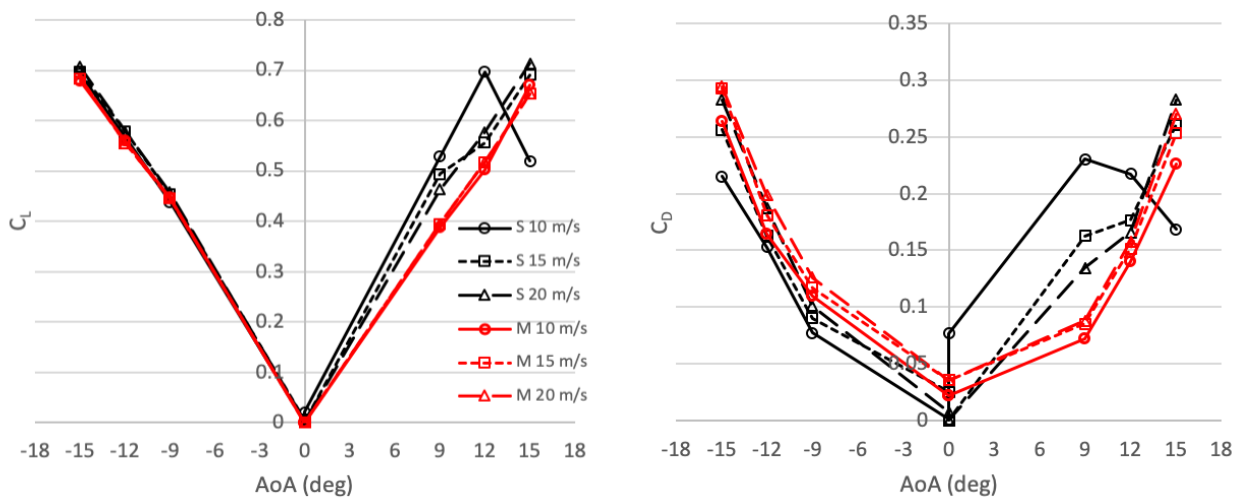
Figure 8 – Comparison of experimental lift and drag coefficients for the solid wing (black) and membrane wing (red).

3. NUMERICAL INVESTIGATIONS

The numerical simulations aimed to replicate the conditions of the wind tunnel experiments and to compare a NACA 0012 foil with one modified to include the measured membrane deformations but not the observed bend and twist.

3.1 Numerical Method

The numerical simulations were performed using Star CCM+ (CD-Adapco, 2016). The simulation domain replicated the 10.5 meter long working section of the wind tunnel facility used in the experiments (Figure 9). The wind tunnel walls had a slip boundary condition whilst the aerofoil had a non-slip condition applied to ensure that the boundary layer would develop.
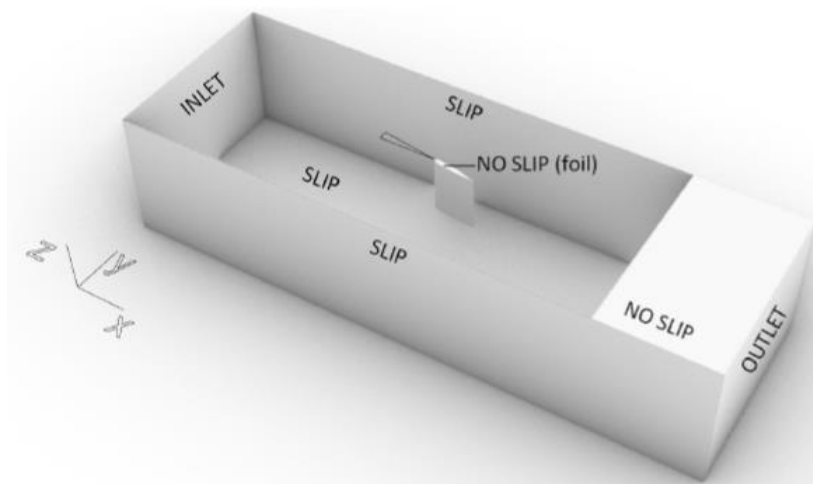

Figure 9 - Simulation domain

The rigid foil geometry was easily created based on the NACA profile from the experimental wing section. Different deformed geometries were required for the membrane wing for each of the tested angles of attack and wind speeds. The measured membrane deformations were used to

81

modify the rigid foil geometry within Rhino, creating a series of deformed foil shapes similar to one provided in Figure 10.
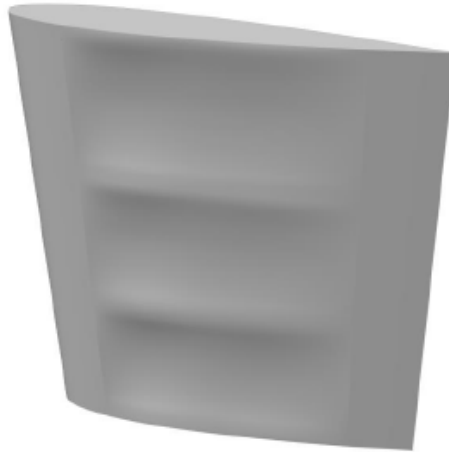

Figure 10 - Deformed membrane geometry for AoA=0 and 10m/s.

The deformations of the top membrane panel were not measured experimentally. Therefore, these were assumed to have been the same as the middle panel as this will not have been affected by the tip effects and the tunnel roof will effectively create a reflection plane. This ignores any potential effects of the tunnel wall boundary layer but these are assumed to be small.

An unstructured mesh was generated within Star CCM providing a base mesh of hexahedral cells with areas of local refinements around the foil and its wake. A prism layer mesh was added to the surface of the foil to create a boundary layer mesh, aligned to the flow direction, with greater levels of control over near wall cell thicknesses.

Various mesh parameters (including: the base cell size, the relative target size, the minimum surface size, the surface curvature, the number and thickness of prism layers) were varied independently to understand their impact on the simulated forces. This resulted in a final mesh structure presented in Figure 11. This provided a total mesh size of 2.4M cells, including 30 prism layers on the foil ensuring the y+ value on the surface of the foil was maintained below 0.5. A mesh sensitivity study, varying the base cell size on this final mesh structure was conducted for the case of 9 degrees angle of attack and a wind speed of 10 m/s. Figure 12 presents the change in force coefficients against the grid characteristic number (R_i), calculated based on the number of cells in the finest mesh (h_1 = 3.7M cells) compared to each individual mesh (h_i):

$$R_i = \sqrt{\frac{h_1}{h_i}}$$

The change in the simulated forces as you approach the finest mesh diminish whilst the computational cost increases rapidly. Therefore the total mesh size of 2.4M cells (the second finest mesh) was used for the numerical investigations.
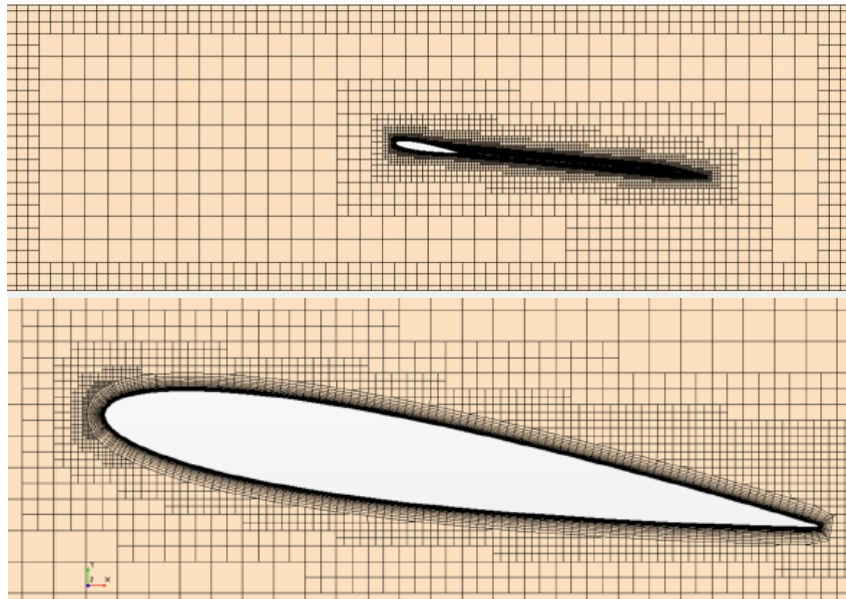
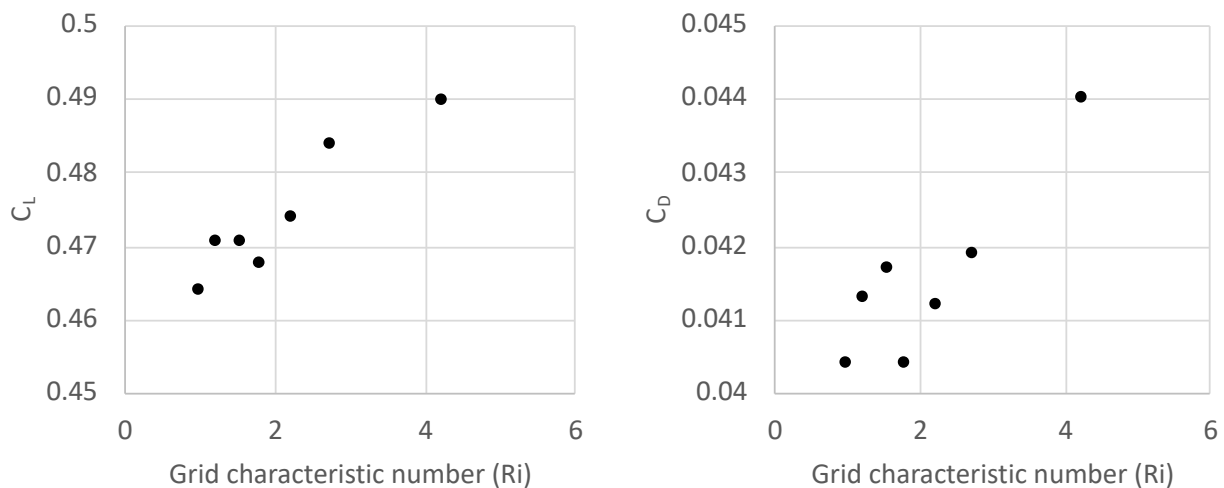**Figure 11 - Final mesh structure around the foil**

Figure 12 - Mesh Sensitivity study

Several different turbulence models were investigated including K-epsilon, Spalart Almaras, standard K-Omega, K-Omega SST and K-omega (gama Re-theta). This indicated that the turbulence model had a significant impact on the forces produced, especially the drag coefficient, with K-epsilon varying significantly from the others. In general the lift coefficient agreed well with the experimental data however all the models produced a drag coefficient significantly lower than the wind tunnel data. Without a definitive answer the K-omega (gama Re-theta) model was selected as it takes into consideration the transition from laminar to turbulent flow and this was likely to be important over the range of tested Reynolds numbers.

3.2 Validation

Before investigating the effect of membrane deformations on the aerodynamic performance the numerical methodology was compared against the experimental data to provide confidence in the results. The rigid aerofoil geometry was simulated at the same angles of attack as the solid foam wing was tested in the wind tunnel. A simulation of the rigid geometry was also conducted using the software xflr5 to provide an additional comparison using a 3D panel method (Xflr5.com, n.d).

83

Figure 13 provides a comparison between the simulated results and the experimental data for negative angles of attack (thus removing the experimental data with unexplained trends in lift and drag). The simulated lift coefficient from CFD is slightly higher than the experimental data, however the simulated drag coefficient is significantly lower than the experimental value measured in the wind tunnel. As previously discussed, the experimental data has additional uncertainty associated with foil alignment and some global deformations associated with twist. This could explain the discrepancies in lift coefficient but would not account for the difference observed in drag.

Previous experimental data for 2D NACA0012 aerofoils indicates a stall angle of approximately 16 degrees but with lift and drag coefficients in the region 1.5 and 0.012 respectively for an angle of attack of 15 degrees (Abbott and Doenhoff, 1959). Obviously the low aspect ratio wing investigated here will have a significantly lower lift coefficient and higher drag coefficient that a 2D section due to 3D affects associated with the tip. A previous study by Yousefi and Saleh (2015) performed a 3D suction flow control study to investigate the aerodynamic characteristics of a rectangular planform NACA0012 wing with an aspect ratio of 2 at a Reynolds number of 500,000. Their CFD results estimated a lift coefficient and drag coefficient of around 0.90 and 0.12 respectively at an angle of attack of 16deg and compared these results to an experiment with similar values. Although not a direct comparison with the wing in this study they do tend to agree with the lower drag coefficient provided by both the CFD and the 3D xflr5 simulations.

One potential reason for the higher drag measured in the wind tunnel could be the effect of the surface finish associated with the membrane, which was stretched over the surface of the solid wing as well as the ribbed wing. Dynamic motions of the membrane, the matt surface finish of the paint or the applied speckle pattern printed transfer could affect the surface roughness which is not modelled in the CFD however this is unlikely to account for such a big difference. It is clear however that the correct trends are observed from the CFD simulations and that this methodology should be able to investigate the relative change in lift and drag and therefore the impact of the membrane deformations on foil performance.

3.3 Results

A series of deformed membrane geometries were simulated for a range of angles of attack and wind speeds with the aerodynamic coefficients compared to those simulated for the solid wing (Table 1). It can be observed that for all non-zero angles of attack the lift increases by a small amount (up to 2%) due to the membrane deformations. Whereas, in general, the drag increased by a greater proportion, especially at the larger wind speeds when larger membrane deformations were measured. This increase in both lift and drag has been demonstrated for membrane wings previously for Micro Aerial Vehicles (MAV) (Arbos Torrent, 2013).

The large percentage increase in drag at zero angle of attack is in part due to a slightly higher absolute increase in drag compared to positive angles of attack but mainly because the total drag for an aerofoil at zero angle of attack is very low. The increase in drag is likely to be associated with increased amounts of flow separation around the areas of high surface curvature especially at the edges of the membrane panels. These local effects can be observed in the pressure distribution along the chord (Figure 14). The largest differences are seen at the leading edge of the membrane panel and it can be seen to affect both the pressure and suction side of the foil.

As the wind speed increases the larger membrane deformations increase the drag by a greater proportion then the lift resulting in a small reduction in the lift to drag ratio. Overall it appears that at lower wind speeds the membrane wing has a similar performance to the solid wing but that as the wind speed increases the membrane wing becomes slightly less efficient. This would make sense with increased membrane deformations at higher wind speeds.
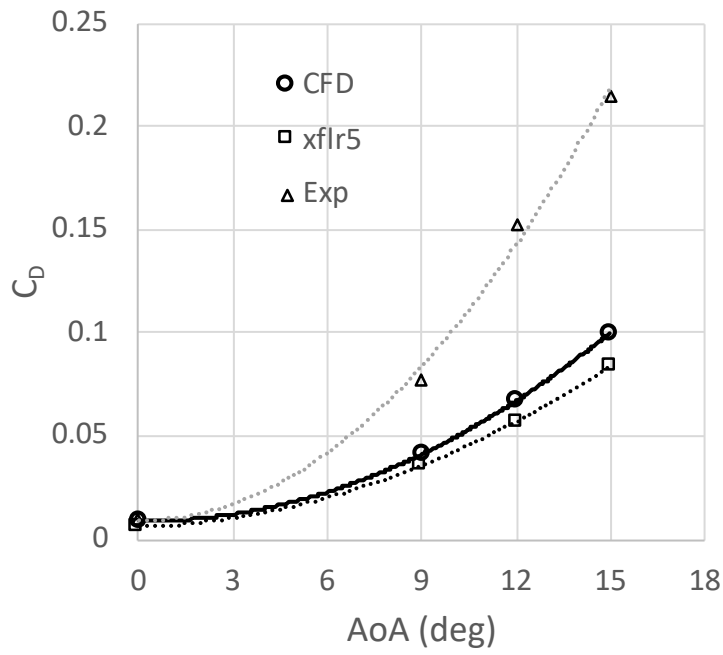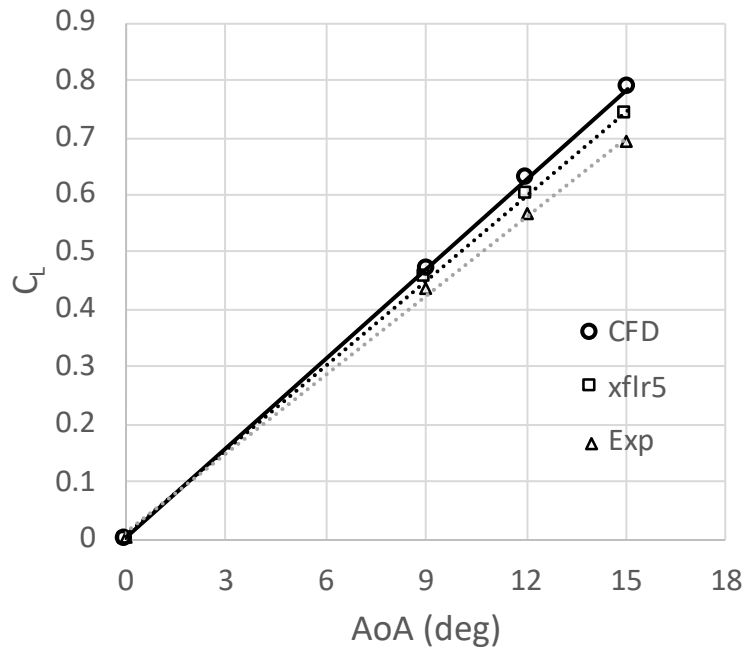
Figure 13 - Comparison between numerical and experimental lift and drag coefficients for the solid wing at a wind speed of 10 m/s. Linear trendlines added for lift and 2nd order polynomial for drag.

Table 1 - Simulated lift and drag coefficient for both configurations with the percentage difference presented for the deformed membrane wing compared to the solid wing.

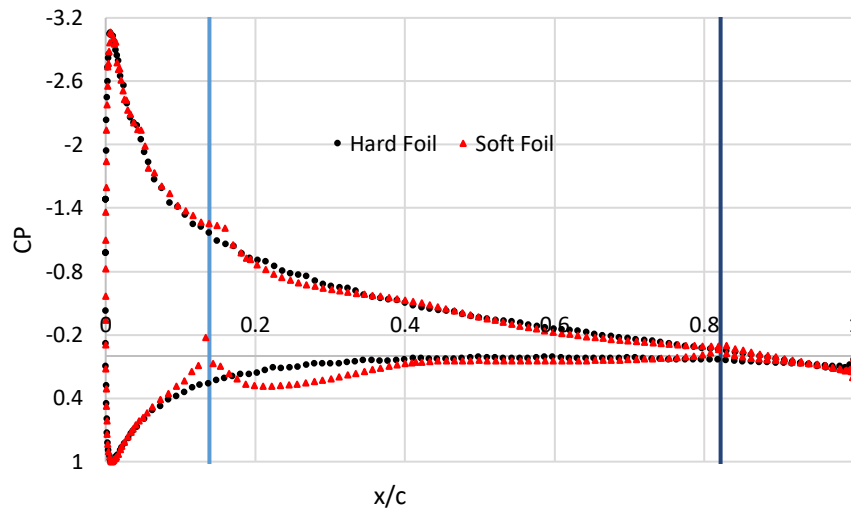| V (m/s)	AOA (°)	Solid Wing		Membrane Wing		ΔCL	ΔCD	Δ(CL/CD)
		CL	CD	CL	CD			
	0	0	0.009	0	0.0105	0.0%	16.7%	0.0%
10	12	0.63	0.067	0.6388	0.0679	1.4%	1.3%	0.1%
	15	0.788	0.1005	0.7922	0.1005	0.6%	0.0%	0.6%
	0	0	0.0082	0	0.0105	0.0%	28.0%	0.0%
15	12	0.634	0.0661	0.6435	0.0677	1.6%	2.4%	-0.7%
	15	0.796	0.0999	0.8073	0.1016	1.4%	1.7%	-0.3%
	0	0	0.0078	0	0.0106	0.0%	35.9%	0.0%
20	12	0.635	0.0654	0.6477	0.0675	2.0%	3.2%	-1.2%
	15	0.803	0.0996	0.8175	0.1028	1.9%	3.2%	-1.3%

Figure 14 – Chordwise pressure distribution at the middle of the span for 20 m/s and 12 degrees AoA. The edges of the membrane panel are indicated by vertical lines.

5. DISCUSSION

Both the experiments and the CFD simulations showed a reduction in foil performance (lift to drag ratio) for the membrane wing over the investigated wind speeds and angles of attack. This reduction in performance, however, was much smaller in the numerical studies. This difference has been mainly attributed to the removal of global deformations of the foil, specifically twist, allowing the impact of the membrane deformations alone to be investigated. Future experiments would benefit from a stiffer foil support structure with an additional load bearing beam located near the training edge to minimise these global deformations in the future.

With a limited amount of tunnel time available the primary focus was to measure the membrane deformations leading to a limited number of angles of attack being considered. From an aerodynamic performance point of view it would be good to conduct a wider range of angles of attack including more repeat runs. The current experimental force data is limited in its ability to effectively correct for foil alignment and provide experimental uncertainty through repeat measurements. This limitation is particularly highlighted by the unusual trends in lift and drag observed for the solid foil at positive angles of attack which can't currently be explained.

The validation of the CFD model showed significantly lower drag then was measured in the wind tunnel despite a range of numerical parameters being investigated including mesh structure, cell density and turbulence modelling. There is limited experimental data published for low aspect ratio NACA0012 wings but Yousefi and Saleh (2015) found drag coefficients similar to the presented CFD values. Future experimental studies are required to investigate the higher drag values observed in the wind tunnel to further understand their origins.

The numerical study seems to suggest that the reduction in foil performance is actually very small given the size of the membrane deformations. This can be in part explained by looking at the pressure distributions plotted in Figure 14. The majority of the pressure differential that generates the lift force is located near the leading edge of the foil which remains a solid foam section. The majority of the impact is therefore likely to be in flow separation increasing the drag.

It is worth highlighting that a small reduction in foil performance can be justified if this results in a significant weight saving. The larger reduction in foil performance observed in the wind tunnel could indicate that the global deformations of a ribbed wing structure could have a larger impact on the foil performance than those of the membrane. Another possible reason for the larger performance differences observed in the wind tunnel could be dynamic membrane motions, which would not be captured in the static CFD geomitries. Although no observation of this phenomenon was made by eye or in the DIC data, previous research into dynamic behaviour of membrane wings indicates that this could have a significant impact on the aerodynamic forces (Rojratsirikul, 2010; Bleischwitz et al, 2017).

This work has focused on relatively large angles of attack however it would be interesting to investigate the impact of these membrane deformations at smaller angles as well. Previous researchers have suggested increased performance is possible from membrane wings and the CFD simulations at lower wind speeds indicate that a very small increase in performance might be possible. Therefore, it would be interesting to investigate if there are operating conditions where an aerodynamic performance benefit could be observed.

6. CONCLUSIONS

This study tested a section of a wing sail, constructed using foam ribs supporting a membrane surface, within the R.J. Mitchel wind tunnel at the University of Southampton. A stereo DIC system was used to measure the membrane deformation over 2/3rds of the wings span on both the pressure and suction side of the aerofoil. This showed that membrane deformations of up to 15%

of the section thickness were observed at the mid-point between foam ribs significantly changing the section shape.

The impact on the aerodynamic performance was determined by comparing the aerodynamic forces with those generated by a solid foam wing with the same dimensions. This indicated an overall reduction in lift to drag ratio of between 5 and 11% depending on which data was included in the analysis. This overall change in performance for the membrane wing includes both the impact of membrane deformations and the global bend and twist deformations observed.

The impact of the static membrane deformations alone was investigated numerically by generating deformed foil geometries for a range of different test conditions based on the experimental measurements. This concluded a reduction in lift to drag ratio of up to 1.3% for the highest wind speeds and angles of attack.

Based on the CFD simulations conducted, it appears that the impact of static membrane displacements on aerofoil performance was small. Larger differences were observed in the wind tunnel, which are thought to be due to greater bend and twist deformations for the ribbed wing structure and possible dynamic membrane deformations. Further experimental studies should be conducted to remove the global deformations and investigate a wider range of angles of attack.

7. ACKNOWLEDGEMENTS

8. REFERENCES

Abbott, I. H. and von Doenhoff, A. E.,(1959). Theory of Wing Sections, Dover Publications, New York.

Arbos Torrent, S. (2013). Aeromechanical performance of compliant aerofoils. PhD Thesis. Imperial College London.

Aubin, N., Augier, B., Sacher, M., Bot, P., Hauville, F. and Flay, R., 2017. Wind tunnel investigation of dynamic trimming on upwind sail aerodynamics. Journal of Sailing Technology, pp.2010-2011.

Banks, J., Marimon Giovannetti, L., Soubeyran, X., Wright, A., Turnock, S., and Boyd, S. (2015). Assessment of digital image correlation as a method of obtaining deformations of a structure under fluid load. Journal of Fluids and Structures, 58, 173-187.

Bleischwitz, R., De Kat, R. and Ganapathisubramani, B. (2016) Aeromechanics of membrane and rigid wings in and out of ground-effect at moderate Reynolds numbers. Journal of Fluids and Structures, 62, pp.318-331.

Bleischwitz, R., de Kat, R., Ganapathisubramani, B. (2017) On the fluid-structure interaction of flexible membrane wings for MAVs in and out of ground-effect. Journal of Fluids and Structures, Volume 70, Pages 214-234,

CD-Adapco (2016). STAR CCM+ Documentation

Collie, S., Fallow, B., Hutchins, N. and Youngren, H. (2015) Aerodynamic design development of AC72 wings. 5th High Performance Yacht Design Conference Auckland.

Deparday, J., Bot, P., Hauville, F., Augier, B. and Rabaud, M., 2016. Full-scale flying shape measurement of offwind yacht sails with photogrammetry. Ocean Engineering, 127, pp.135-143.

Fairuz, Z., Abdullah, M., Zubair, M., Abdul Mujeebu, M., Abdullah, M., Yusoff, H. and Abdul Aziz, M. (2016). Effect of wing deformation on the aerodynamic performance of flapping wings: fluid structure interaction approach. Journal of Aerospace Engineering, 29(4). p.04016006.

Fiumara, A., Gourdai, N., Chapin, V. and Senter, J. (2016). Aerodynamic analysis of 3D multi elements wings: an application to wing sails of flying boats. Royal Aeronautical Society. Applied Aerodynamic Conference. Bristol. UK

Fiumara, A., Gourdai, N., Chapin, V., Senter, J. and Yannick, B., (2016b). Numerical and experimental analysis of the flow around a two-element wingsail at Reynolds number 0.53 × 106. International Journal of Heat and Fluid Flow, vol. 62. pp. 538-551. ISSN 0142-727X

Furukawa, H., Blakeley, A.W., Flay, R,, Richards, P. (2015) Performance of wing sail with multi element by two-dimensional wind tunnel investigations. Journal of Fluid Science and Technology, 10 (2).

Gordnier, R.E. and Attar, P.J. (2014) Impact of flexibility on the aerodynamics of an aspect ratio two membrane wing, Journal of Fluids and Structures, Volume 45, Pages 138-152.

Haack, N. (2018). C-class catamaran wing performance optimization. MPhil Thesis. University of Manchester. Available at: http://cfd.mace.manchester.ac.uk/twiki/pub/CfdTm/ResPub261/thesis.pdf [Accessed 13 Apr. 2018].

Hagemeister, N. and Flay, R.G. (2019) Velocity Prediction of Wing-Sailed Hydrofoiling Catamarans. Journal of Sailing Technology, 4(01), pp.66-83.

Hansen, H., Hochkirch, K., Burns, I. and Ferguson, S. (2019) Maneuver Simulation and Optimization for AC50 Class. Journal of Sailing Technology, 4(01), pp.142-160.

Jackson, P.S., Johnston, M.S. and Flay, R.G. (2001) Some Aspects of the Aerodynamics of Membrane Wings. In 14th Australasian Fluid Mechanics Conference (pp. 10-14).

Li, C., Wang, H. and Sun, P., (2020) Numerical Investigation of a Two-Element Wingsail for Ship Auxiliary Propulsion. Journal of Marine Science and Engineering, 8(5), p.333.

Magherini, M., Turnock, S.R. and Campbell, I.M.C. (2014) Parameters affecting the performance of the c-class wingsail. International Journal of Small Craft Technology, 156(B1), pp.21-34.

Marimon Giovannetti, L., Banks, J., Turnock, S., and Boyd, S.,(2017). Uncertainty assessment of coupled Digital Image Correlation and Particle Image Velocimetry for fluid-structure interaction wind tunnel experiments. Journal of Fluids and Structures, 68, 125-140.

Olsson, F., Giovannetti, L., Werner, S. and Finnsgård, C. (2020) A Performance Depowering Investigation for Wind Powered Cargo Ships Along a Route. Journal of Sailing Technology, 5(01), pp.47-60.

Piquee, J., López Canalejo, I., Breitsamter, C. et al. Aerodynamic analysis of a generic wing featuring an elasto-flexible lifting surface. Adv. Aerodyn. 1, 20 (2019). https://doi.org/10.1186/s42774-019-0022-7

Ramolini, A., 2019. Implementation of a Fluid-Structure Interaction Solver for a Spinnaker Sail. Journal of Sailing Technology, 4(01), pp.1-16.

Rojratsirikul, P. (2010) Aerodynamics of flexible membranes. Doctoral Thesis. University of Bath.

Viola, IM, Biancolini, ME, Sacher, M & Ubaldo, C (2015) A CFD-based wing sail optimisation method coupled to a VPP, 5th High Performance Yacht Design Conference, Auckland, New Zealand, 9/03/15 - 11/03/15.

Xflr5.com. (n.d.). Xflr5: Results vs Prediction. [online] Available at: http://www.xflr5.com/docs/Results_vs_Prediction.pdf [Accessed 21 Sep. 2018].

Yousefi, K. and Saleh, R. (2015). Three-dimensional suction flow control and suction jet length optimization of NACA 0012 wing. Meccanica, Springer Verlag, 50 (6), pp.1481-1494.